Disclaimer

This note has not been internally reviewed by the DØ Collaboration. Results or plots contained in this note were only intended for internal documentation by the authors of the note and they are not approved as scientific results by either the authors or the DØ Collaboration. All approved scientific results of the DØ Collaboration have been published as internally reviewed Conference Notes or in peer reviewed journals.

CERN – TH – 4846/87 D0– 624
September 1987
Preliminary Version

Limits on CP Violating Asymmetries from $B^0\bar{B}^0$ Mixing Results.

PAULA J. FRANZINI

CERN – Geneva

ABSTRACT

In view of the recent measurements of $B_d^0\bar{B}_d^0$ mixing, and of ϵ'/ϵ, we calculate the $B^0\bar{B}^0$ mixing asymmetries. We find that the constraint of these observations greatly decreases the allowed range of the parameters a, the dilepton charge asymmetry, and $l^{\pm}$, the total lepton charge asymmetry. We conclude that almost certainly $a < 2.7 \times 10^{-3}$ and $l^{\pm} < 6 \times 10^{-4}$ for $m_t = 45$ GeV; for bigger m_t the bounds become even smaller.

1. Introduction

While many previous authors (see for example ref.s $1-4$) have estimated the CP violating effects in $B\bar{B}$ mixing, the constraints imposed by two new measurements, namely of $B_d^0\bar{B}_d^0$ mixing by the ARGUS collaboration at DESY,[5] and of ϵ'/ϵ by the NA31 collaboration at CERN,[6] merit a new look at the situation. Both of these measurements, with their preference for large m_t, point to small expected standard model values for the CP violating effects in $B\bar{B}$ physics. Explicit calculations show that even for large m_t the mixing measurement puts further constraints on a. Thus any asymmetries in the mixing observed at the next generation of experiments will almost certainly be a signature of "new physics."

In this paper, we present a statistical analysis of the predicted ranges of the CP violating asymmetries, the mixing, and m_t, the top mass. We randomize the unknown inputs — the Kobayashi-Maskawa (KM) angles, the "bag" parameter B_B, the B lifetime τ_B, and so on — within their current limits, and calculate the resulting distributions in the asymmetries and the mixing for various values of m_t. The results are presented in the form of selected histograms, and a table of the values at which 10% or 1% of the sample remains, before and after the constraints from the measured values of ϵ, ϵ'/ϵ, and mixing. In Section 2 we set forth the relevant equations on which our calculations are based; in Section 3 we summarize the constraints, and in Section 4 we present our results on the predicted ranges of the asymmetry parameters, the mixing, and the top quark mass.

2. Basic Formulas

We start by defining a few fundamental quantities—the mixing parameters, r and $\bar{r}$:[7]

$$r \equiv \frac{P(B^0 \to l^+\nu X^-)}{P(B^0 \to l^-\bar{\nu}X^+)} = \eta^2 \frac{x^2+y^2}{2+x^2-y^2} \approx \eta^2 \frac{x^2}{2+x^2} \tag{2.1}$$

$$\bar{r} \equiv \frac{P(\bar{B}^0 \to l^-\bar{\nu}X^+)}{P(\bar{B}^0 \to l^+\nu X^-)} = \eta^{-2} \frac{x^2+y^2}{2+x^2-y^2} \approx \eta^{-2} \frac{x^2}{2+x^2}; \tag{2.2}$$

the numbers of dilepton pairs observed, l^{++} etc., due to production, subsequent mixing, and decay of $B^0\bar{B}^0$ pairs in e^+e^- annihilation, of appropriate charges; and the total number of positively (negatively) charged primary leptons, $l^{+(-)}$, coming from the decays of $B^0\bar{B}^0$ pairs. We make the generally used simplifying assumption that there is no CP violation in the semi-leptonic decays of the B mesons, i.e. $BR(B^0 \to l^- + \cdots) = BR(\bar{B}^0 \to l^+ + \cdots)$ (where here the B's and $\bar{B}$'s denote final states after mixing, just prior to decay).[8] Then

the definition

$$r \equiv \frac{P(B^0 \to \bar{B}^0)}{P(B^0 \to B^0)} \tag{2.3}$$

is equivalent to eq. (2.1) and similarly for $\bar{r}$. Here P denotes probability; $x = \Delta M/\Gamma$, $y = \Delta\Gamma/2\Gamma$ with $\Delta M = M_L - M_S$, $\Delta\Gamma = \Gamma_L - \Gamma_S$ and $\Gamma = (\Gamma_S + \Gamma_L)/2$ (where L and S stand for long and short lifetime mass eigenstates); y^2 can be neglected in the B system. η is given in terms of the CP impurity parameter ϵ by $\eta = |(1-\epsilon)/(1+\epsilon)|$. The l's are related by the expressions

$$l^+ = (2l^{++} + l^{+-} + l^{-+})/BR_l \qquad l^- = (2l^{--} + l^{+-} + l^{-+})/BR_l \tag{2.4}$$

where $BR_l = BR(B^0 \to l^+ + \cdots)$; here again B denotes final state after mixing.

We consider three cases:

a) $B\bar{B}$ produced incoherently, as occurs at energies sufficiently above the b flavor threshold. In this case l^{++} and so on are given by

$$l^{++} = N(B^0 \to l^+) \times N(\bar{B}^0 \to l^+)/N \tag{2.5}$$

where N is the initial number of $B\bar{B}$ pairs, and we have the relations

$$r = \frac{l^{++}}{l^{-+}} = \frac{l^{+-}}{l^{--}} \qquad \bar{r} = \frac{l^{--}}{l^{-+}} = \frac{l^{+-}}{l^{++}}. \tag{2.6}$$

From these we derive the measured mixing parameter

$$r_2 \equiv \frac{l^{++} + l^{--}}{l^{++} + l^{+-} + l^{-+} + l^{--}} = \frac{r + \bar{r}}{1 + r + \bar{r} + r\bar{r}} \tag{2.7}$$

the dilepton charge asymmetry,

$$a \equiv \frac{l^{++} - l^{--}}{l^{++} + l^{--}} = \frac{r - \bar{r}}{r + \bar{r}} = \frac{\eta^4 - 1}{\eta^4 + 1}; \tag{2.8}$$

and the total lepton charge asymmetry,

$$l_1^{\pm} \equiv \frac{l^+ - l^-}{l^+ + l^-} = \frac{l^{++} - l^{--}}{l^{++} + l^{--} + l^{+-} + l^{-+}} = \frac{r - \bar{r}}{r + \bar{r} + r\bar{r} + 1}. \tag{2.9}$$

These expressions are given in ref. 3(except that the expression for $l^{\pm}$ given there is that of eq. (2.12)).

b) $B\bar{B}$ produced coherently with $L = 1$. This is the case for experiments done at the $\Upsilon(4S)$ resonance, such as ARGUS and CLEO. In this case one considers the evolution of the state $|B\rangle|\bar{B}\rangle - |\bar{B}\rangle|B\rangle$, rather than B and $\bar{B}$ separately. One finds then the relations

$$r = \frac{l^{++}}{l^{+-}} = \frac{l^{++}}{l^{-+}} \qquad \bar{r} = \frac{l^{--}}{l^{+-}} = \frac{l^{--}}{l^{-+}} \tag{2.10}$$

from which one gets

$$r_2 = \frac{r + \bar{r}}{2 + r + \bar{r}} \tag{2.11}$$

and

$$l_2^{\pm} = \frac{r - \bar{r}}{2 + r + \bar{r}} \tag{2.12}$$

as in ref. 4. Note that the asymmetry a remains unchanged.

c) Finally, we also consider the case where $B\bar{B}$ is produced coherently in an $L =$ even state. This could happen through $B^*\bar{B}$ production and decay to $B\bar{B}\gamma$ (at energies where this could occur one will actually deal with a mixture of $L =$ odd and $L =$ even states). For $L =$ even we use (rather complicated) expressions for l^{++}, and so on, given in the appendix of ref. 1, and determine $l_3^{\pm}$ accordingly; again, a is unchanged.

To calculate the mixings and asymmetries, we use the following formulae

$$\eta = \left|\frac{1-\epsilon}{1+\epsilon}\right| = \left|\frac{\sqrt{M_{12}^* - i\Gamma_{12}^*/2}}{\sqrt{M_{12} - i\Gamma_{12}/2}}\right| \tag{2.13}$$

where $M_{12} - i\Gamma_{12}/2$ is the off-diagonal element in the $B^0\bar{B}^0$ mass matrix, given by

$$M_{12}(\bar{B}_p^0 \to B_p^0) = \frac{G_F^2 B_{B_p} f_B^2 m_B^{(p)} M_W^2}{12\pi^2}[\lambda_c^{(p)2} U_1 \eta_1^{(B)} + \lambda_t^{(p)2} U_2 \eta_2^{(B)} + 2\lambda_c^{(p)}\lambda_t^{(p)} U_3 \eta_3^{(B)}] \tag{2.14}$$

and

$$\Gamma_{12}(\bar{B}_p^0 \to B_p^0) = \frac{G_F^2 B_{B_p} f_B^2 m_B^{(p)} M_W^2}{8\pi}[\lambda_c^{(p)2} U_4 + \lambda_t^{(p)2} U_5 + 2\lambda_c^{(p)}\lambda_t^{(p)} U_6]. \tag{2.15}$$

Here p stands for d or s, f_B is the B-meson decay parameter, B_{B_p} is the "bag" parameter, and $m_B^{(p)}$ is the mass of the B_p^0 meson. The $\eta_i^{(B)}$ are QCD corrections. The λ_i are given

by

$$\lambda_i^{(p)} = V_{ib}^* V_{ip} \qquad i = u, c, t \tag{2.16}$$

and for the Kobayashi-Maskawa[9] matrix elements V_{ij} we take the approximate parame-tri-za-tion[10]

$$V = \begin{pmatrix} V_{ud} & V_{us} & V_{ub} \\ V_{cd} & V_{cs} & V_{cb} \\ V_{td} & V_{ts} & V_{tb} \end{pmatrix} \approx \begin{pmatrix} 1 - \frac{1}{2}\lambda^2 & \lambda & A\lambda^3 \rho e^{i\phi} \\ -\lambda & 1 - \frac{1}{2}\lambda^2 & A\lambda^2 \\ A\lambda^3(1 - \rho e^{-i\phi}) & -A\lambda^2 & 1 \end{pmatrix}. \tag{2.17}$$

The U_i's are functions of m_u, m_c, m_b, m_t and M_W given in ref. 4; for this paper we use $U_1 = 3.28 \times 10^{-5}$; U_2 as given by the approximate formula $S(x_c, x_t)$ in ref. 11; $U_3 = 1.3 \times 10^{-3}$ (the slight dependence of U_3 on m_t can be ignored in view of the minor role that U_3 plays in our calculations); $U_4 = -.129$; $U_5 = 23.3$; and $U_6 = 2.41$ (U_4, U_5 and U_6 are functions of m_b, m_c and various QCD parameters).

And finally, we use

$$\Delta M = \sqrt{2}\sqrt{\sqrt{d_1^2 + d_2^2} + d_1} \tag{2.18}$$

where $d_1 = |M_{12}|^2 - |\Gamma_{12}|^2/4$ and $d_2 = -Re(M_{12}\Gamma_{12}^*)$. We have checked that the possible uncertainties of the parameters η_1, η_2, η_3, U_1, U_2, U_3, and the QCD corrections on which U_4, U_5 and U_6 depend lead to errors of at most a few percent. The greatest uncertainty lies in the assumptions $m_c = 1.4$ GeV and $m_b = 4.6$ GeV inherent in the values used for the U_i. Increasing m_c to 1.7 GeV causes a 50% rise in a (and has no effect on r); increasing m_b has a much smaller, opposing effect.

The remaining variables are now the KM/Wolfenstein parameters A, ρ, and ϕ (we take $\lambda = .221$), and $B_B f_B^2$, m_t and τ_B. In section 4 we present our results on the possible range of the asymmetries in the B_d system given the uncertainties in these parameters.

3. Constraints

We will consider various combinations of three constraints:

a) $$\epsilon = (2.28 \pm .05) \times 10^{-3} \tag{3.1}$$

The theoretical value of ϵ is calculated from the expression

$$|\epsilon| = \frac{\mathrm{Im}M_{12} + \xi(2\mathrm{Re}M_{12})}{\sqrt{2}\Delta m_K} = \frac{G_F^2 M_W^2}{12\sqrt{2}\pi^2} \frac{B_K f_K^2 m_K}{\Delta m_K}(D + 2\xi F) \tag{3.2}$$

where the kernels D and F are specified in eqs. (2.12) and (2.13) of ref. 11. D is

proportional to $\mathrm{Im}(V_{td}^* V_{ts}) = A^2\lambda^5\rho\sin\phi$ and ξ is given by

$$\xi = -.54A^2\lambda^4\rho\sin\phi. \tag{3.3}$$

We use $f_K = 160$ MeV, $\Delta m_K/m_K = .71 \times 10^{-14}$ and $B_K = 1$. Unless otherwise stated, we constrain ϵ to lie between 2.19×10^{-3} and 2.37×10^{-3} —i.e., the 1.64σ or 90% percent confidence limits.

b) $$\frac{\epsilon'}{\epsilon} = (3.5 \pm .4 \pm .7 \pm 1.2) \times 10^{-3} = (3.5 \pm 1.45) \times 10^{-3} \tag{3.4}$$

if we combine the three errors in quadrature. To calculate ϵ'/ϵ we use the expression[12]

$$\frac{\epsilon'}{\epsilon} = 15.6\xi. \tag{3.5}$$

Unless otherwise stated, we require that this calculated number agree to within a factor of two (to account for theoretical uncertainties) with the 1.64σ limits of the experimental number; in other words we constrain ξ to lie between $.036 \times 10^{-3}$ and $.75 \times 10^{-3}$. We also consider the constraints imposed if we instead use 1σ limits.

c) $$x_d = .73 \pm .18 \tag{3.6}$$

Unless otherwise stated, we require the calculated value of x_d to lie between .43 and 1.03, the 1.64σ limits.

4. Results: ranges of asymmetries, mixing, m_t

In ref. 13 the allowed ranges of the parameters relevant to $B\bar{B}$ mixing were discussed, and the amount of mixing calculated for a few different values of these parameters, particularly extremal ones. In this paper we have chosen the less conventional approach of randomly selecting values for these parameters within their allowed ranges, and calculating the resultant distribution of the quantities we are interested in, a and $l^{\pm}$. While this method is rather qualitative, since what distributions should be chosen is rather unclear, choosing extremal values for input parameters to determine limits is also uncertain, as one may judge from the range of values arrived at for, e.g., limits on m_t from the Argus mixing measurement.[14] Moreover, this crude Monte Carlo technique has the advantage of lending itself well to the imposing of constraints, such as the measured values of ϵ, $\frac{\epsilon'}{\epsilon}$, and x_d.

We shall show results for one main set of initial parameter distributions, as well as give an example of the variation in results caused by varying the input distributions. This set consists of flat distributions of most of the parameters (whose uncertainties are in significant part theoretical) in ranges somewhat wider than those given in ref.13. The B lifetime is taken with a Gaussian distribution. Thus:

$$\begin{aligned} \textit{Set A} \quad & \tau_B = 1.11 \pm .16 \text{ ps (gaussian)}; \quad A = (.92 \text{ to } 1.52)/(\tau_B \text{ in } ps) \\ & B_B f_B^2 = 90 \text{ to } 190\text{MeV} \\ & R = 0 \text{ to } 0.9 \quad \phi = 0 \text{ to } \pi \end{aligned}$$

Fig. 1 is a scatter plot of a_d versus x_d for $m_t = 45$ GeV, to illustrate the restriction imposed by the mixing result. In Fig. 2 we histogram the number of points per bin in a_d, for a total sample of 1000 points. The solid line is the distribution prior to imposing any constraints; the dashed line is the distribution after imposing the ϵ and ϵ'/ϵ constraints; and the dotted line is that after both ϵ and mixing constraints (imposing all three constraints gives the identical result). We do not illustrate the results of imposing the ϵ constraint alone; it shifts the distribution away from the origin so that it peaks around $a = .003$ and is somewhat higher from $a = .005$ to .01; beyond this region it has negligible effect.

In Fig. 3, for $m_t = 80$ GeV, we show the distributions for no constraints; ϵ and ϵ'/ϵ; and ϵ and mixing. Here, instead, ϵ by itself gives a histogram that is almost identical to that given by ϵ and ϵ'/ϵ together; by $m_t = 110$ GeV, to our accuracies, the results are completely identical. A similar histogram in x_d would show agreement with ref.13 in that for $m_t = 45$ GeV the observed mixing value is virtually excluded, while for $m_t = 60$ GeV it is moderately unlikely (at the 10% level).

The effects of the constraints on the top mass is made more clear if we also randomize m_t (we choose a flat distribution in the range 40 GeV to 180 GeV), and then histogram the values of m_t corresponding to allowed data points. Thus in Fig. 4 we show histograms of m_t subject to the ϵ constraint alone (solid); the ϵ and ϵ'/ϵ constraints (dashed); and for all three constraints (or identically for just ϵ and mixing) in dots. The distribution before any cuts would correspond to a horizontal straight line at $\#\ of\ pt.s = 35.7$.

In all these distributions we have collected one thousand points *after* constraints; the number of points before constraints is given in Table 1. The fact that for small m_t we must look at a very large number of points before finding 1000 that satisfy all the constraints does not *a priori* make small m_t statistically unlikely. It merely means that if m_t is small, a large part of the previously allowed region in parameter space has been made unphysical by the constraints of new observations—the measurement has essentially determined the remaining parameters. However, this small percentage of viable points is generally associated with many inputs being simultaneously pushed to their extreme values; this would still not be statistically any more unlikely than any other set of input parameters, except that the likelihood of most of the inputs presumably falls off towards the endpoints of the intervals chosen.

The rest of our results are given in Tables 2-7, where we have given the 10% and 1% levels for x_d, a and the three $l^{\pm}$'s for different sets of initial parameter distributions, constraints, and values of m_t. In Table 7 we give the results for variable m_t.

To illustrate the variations inherent to this method, we give results for a second set of assumptions:

$$Set\ B \quad \tau_B = .91 \text{ to } 1.31 \text{ ps (flat)}; \quad \cos\phi = -1 \text{ to } 1 \text{ ps (flat)}$$

(other parameters as before). For this set we consider 2.6σ (99%$c.l.$) constraints for ϵ, and 1σ constraints for mixing and ϵ'/ϵ. We choose $m_t = 60$ GeV for illustration. The values of a are 20% lower; there are no significant qualitative differences. We have also looked at the effect of changing the range of τ_B to be $1.18 \pm .14$ ps in accordance with the latest measurements[15] and find that it lowers our numbers for x and $l^{\pm}$ by at most 10%, leaving a unchanged, before cuts; after constraining the mixing, it lowers a and $l^{\pm}$ by at most 10%.

	ϵ	$\frac{\epsilon'}{\epsilon}$	$\epsilon + \frac{\epsilon'}{\epsilon}$	$\epsilon +$ mixing
(Set A)				
$m_t = 110$ GeV	52	1.5	52	150
$m_t = 80$ GeV	45	—	45	230
$m_t = 60$ GeV	43	—	52	432
$m_t = 45$ GeV	53	—	118	1751
$40 < m_t < 180$ GeV	48	—	50	208
(Set B)				
$m_t = 60$ GeV	22	—	35	1144

Table 1 . Total number of points (in units of thousands) before constraints for each histogram

Constraints	Upper Limits		Lower Limits	
	1%	10%	1%	10%
(Set A; $m_t = 110$ GeV)				
none	7.4	2.8	.007	.096
ϵ	8.1	3.7	.07	.18
$\frac{\epsilon'}{\epsilon}$	8.	2.9	.04	.14
ϵ + mixing	1.45	.825	.062	.14
$\frac{\epsilon'}{\epsilon}$ + ϵ same as ϵ alone				
(Set A; $m_t = 60$ GeV)				
none	20.	7.5	.02	.255
ϵ	16.25	8.5	.35	.875
$\epsilon + \frac{\epsilon'}{\epsilon}$	8.9	5.3	.31	.76
ϵ + mixing	2.17	1.52	.19	.385
$\frac{\epsilon'}{\epsilon}$ + ϵ + mixing same as ϵ + mixing for this and following cases				
(Set A; $m_t = 45$ GeV)				
none	32.5	12.5	.03	.415
ϵ	20.7	11.5	.62	1.7
$\epsilon + \frac{\epsilon'}{\epsilon}$	7.4	4.7	.68	1.36
ϵ + mixing	2.67	2.02	.42	.62
(Set B; $m_t = 60$ GeV)				
none	16.6	6.5	.075	.5
ϵ	13.3	7.25	.57	1.15
$\epsilon + \frac{\epsilon'}{\epsilon}$	5.6	3.6	.53	.98
ϵ + mixing	1.53	1.17	.31	.47

Table 2 . Limits on $a \times 10^3$

Constraints	Upper Limits		Lower Limits	
	1%	10%	1%	10%
(Set A; $m_t = 110$ GeV)				
none	2.47	1.19	.018	.099
ϵ	1.82	.89	.045	.1
$\frac{\epsilon'}{\epsilon}$	2.28	1.04	.015	.088
$\frac{\epsilon'}{\epsilon}$ + ϵ same as ϵ alone				
(Set A; $m_t = 60$ GeV)				
none	.92	.44	.007	.037
ϵ	.755	.42	.03	.061
$\epsilon + \frac{\epsilon'}{\epsilon}$	.85	.46	.04	.086
(Set A; $m_t = 45$ GeV)				
none	.56	.27	.004	.022
ϵ	.53	.30	.027	.051
$\epsilon + \frac{\epsilon'}{\epsilon}$	.62	.37	.048	.087
(Set B; $m_t = 60$ GeV)				
none	.73	.40	.018	.058
ϵ	.57	.36	.031	.065
$\epsilon + \frac{\epsilon'}{\epsilon}$	.71	.42	.055	.097

Table 3 . Limits on x

Constraints	Upper Limits		Lower Limits	
	1%	10%	1%	10%
(Set A; $m_t = 110$ GeV)				
none	6.35	3.4	.005	.055
ϵ	2.62	1.52	.082	.19
$\frac{\epsilon'}{\epsilon}$	3.37	2.	.01	.095
ϵ + mixing	2.65	1.77	.165	.35
$\frac{\epsilon'}{\epsilon}$ + ϵ same as ϵ alone				
(Set A; $m_t = 60$ GeV)				
none	7.9	2.5	.002	.024
ϵ	3.1	2.02	.085	.19
$\epsilon + \frac{\epsilon'}{\epsilon}$	3.15	2.17	.085	.22
ϵ + mixing	3.7	2.77	.45	.9
$\frac{\epsilon'}{\epsilon}$ + ϵ + mixing same as ϵ + mixing for this and following cases				
(Set A; $m_t = 45$ GeV)				
none	6.25	1.7	.0015	.014
ϵ	3.6	2.2	.09	.19
$\epsilon + \frac{\epsilon'}{\epsilon}$	3.67	2.4	.12	.23
ϵ + mixing	4.32	3.4	.92	1.32
(Set B; $m_t = 60$ GeV)				
none	7.2	3.1	.009	.06
ϵ	3.02	1.97	.09	.19
$\epsilon + \frac{\epsilon'}{\epsilon}$	2.97	2.05	.11	.22
ϵ + mixing	3.5	2.82	.8	1.22

Table 4 . Limits on $l_1^{\pm} \times 10^4$

Constraints	Upper Limits		Lower Limits	
	1%	10%	1%	10%
(Set A; $m_t = 110$ GeV)				
none	4.5	2.25	.0025	.03
ϵ	1.53	.87	.042	.099
$\frac{\epsilon'}{\epsilon}$	2.15	1.2	.005	.05
ϵ + mixing	1.55	1.05	.094	.2
$\frac{\epsilon'}{\epsilon}$ + ϵ same as ϵ alone				
(Set A; $m_t = 60$ GeV)				
none	4.5	1.4	.001	.012
ϵ	1.8	1.07	.042	.09
$\epsilon + \frac{\epsilon'}{\epsilon}$	1.67	1.17	.042	.11
ϵ + mixing	2.07	1.62	.24	.49
$\frac{\epsilon'}{\epsilon}$ + ϵ + mixing same as ϵ + mixing for this and following cases				
(Set A; $m_t = 45$ GeV)				
none	1.97	1.1	.045	.097
ϵ	3.25	.9	.001	.007
$\epsilon + \frac{\epsilon'}{\epsilon}$	2.05	1.3	.06	.12
ϵ + mixing	2.45	1.9	.52	.72
(Set B; $m_t = 60$ GeV)				
none	4.15	1.65	.0045	.03
ϵ	1.6	1.03	.046	.095
$\epsilon + \frac{\epsilon'}{\epsilon}$	1.6	1.11	.056	.11
ϵ + mixing	2.02	1.67	.47	.72

Table 5 . Limits on $l_2^{\pm} \times 10^4$

Constraints	Upper Limits		Lower Limits	
	1%	10%	1%	10%
(Set A; $m_t = 110$ GeV)				
none	8.5	4.6	.007	.079
ϵ	3.8	2.2	.125	.27
$\frac{\epsilon'}{\epsilon}$	4.6	2.85	.015	.13
ϵ + mixing	3.8	2.5	.23	.49
$\frac{\epsilon'}{\epsilon}$ + ϵ same as ϵ alone				
(Set A; $m_t = 60$ GeV)				
none	11.4	3.7	.003	.036
ϵ	4.5	2.95	.125	.28
$\epsilon + \frac{\epsilon'}{\epsilon}$	4.6	3.2	.13	.33
ϵ + mixing	5.35	3.95	.65	1.3
$\frac{\epsilon'}{\epsilon}$ + ϵ + mixing same as ϵ + mixing for this and following cases				
(Set A; $m_t = 45$ GeV)				
none	9.3	2.6	.002	.022
ϵ	5.2	3.2	.135	.29
$\epsilon + \frac{\epsilon'}{\epsilon}$	5.35	3.6	.18	.35
ϵ + mixing	6.1	4.95	1.35	1.9
(Set B; $m_t = 60$ GeV)				
none	10.1	4.5	.013	.087
ϵ	4.5	2.9	.14	.285
$\epsilon + \frac{\epsilon'}{\epsilon}$	4.35	2.97	.165	.33
ϵ + mixing	4.95	4.	1.15	1.75

Table 6 . Limits on $l_3^{\pm} \times 10^4$

Constraints	m_t	a	x	$l_1^{\pm}$	$l_2^{\pm}$	$l_3^{\pm}$
none	179.(166.)	15.(4.5)	3.6(1.3)	6.6(3.)	4.6(1.9)	9.2(4.1)
	41.(54.)	.007(.09)	.02(.08)	.005(.06)	.003(.03)	.008(.08)
ϵ	179.(164.)	14.(5.5)	2.3(.98)	2.6(1.6)	1.4(.88)	3.8(2.3)
	43.(52.)	.04(.15)	.04(.08)	.08(.18)	.04(.09)	.12(.26)
$\epsilon + \frac{\epsilon'}{\epsilon}$	179.(166.)	8.6(3.9)	2.6(.98)	2.7(1.6)	1.5(.89)	3.8(2.3)
	44.(62.)	.04(.14)	.05(.10)	.08(.17)	.04(.09)	.10(.25)
$\epsilon +$ mixing	179.(166.)	1.6(.85)	1.0(.93)	2.9(1.8)	1.6(1.0)	4.1(2.5)
	53.(77.)	.04(.10)	.43(.46)	.13(.26)	.08(.15)	.19(.36)
$\frac{\epsilon'}{\epsilon} + \epsilon +$ mixing same as $\epsilon +$ mixing						

Table 7 . Limits on m_t, $a \times 10^{-3}$, x_d, and $l^{\pm}_{1,2,3} \times 10^{-4}$ for variable m_t. For each constraint, we specify the 1%(10%) upper limits on the first line, and the 1%(10%) lower limits on the second line.

5. B_s Asymmetries

In order to calculate the analogous asymmetries for B_s mesons, we must go to higher order in λ in the expansion of the KM matrix. Requiring that the imaginary part of the unitarity be satisfied to order λ^4 and the real part to only λ^2 (CP-violating effects being due to the imaginary part) the relevant term is:[16]

$$V_{cb} = A\lambda^2(1 - i\rho \sin\phi\lambda^2). \tag{5.1}$$

The CP violating effects for B_s are of opposite sign and of smaller magnitude, relative to B_d, because they are present only in the charm quark contribution, while B_d is dominated by the top quark contribution. The magnitude of the effect is shown in Table 8, analogous to Table 7. These numbers give a sense for what the dilution in asymmetries due to B_s, which are not separable from B_d at high energies, will be. Of course, to calculate this dilution properly, one must redo the calculation of the asymmetries for appropriate mixtures of B_s and B_d. We note that the effect of the CP violating term in the charm quark contribution for B_d alone is to lower our previous values for asymmetries by $2-3\%$.

Constraints	a	x	$l_1^{\pm}$	$l_2^{\pm}$	$l_3^{\pm}$
none	.46(.19)	35.(19.5)	2.2(.9)	2.(.8)	2.5(1.)
	.0005(.005)	1.(2.2)	.002(.03)	.002(.03)	.002(.03)
ϵ	.5(.2)	34.(17.6)	2.1(1.)	1.9(.82)	2.6(1.1)
	.003(.009)	1.(2.1)	.015(.04)	.015(.04)	.015(.04)
$\epsilon + \frac{\epsilon'}{\epsilon}$	.29(.15)	30.(17.)	1.4(.74)	1.1(.66)	1.6(.82)
	.003(.008)	1.2(2.6)	.015(.04)	.015(.04)	.015(.04)
$\epsilon +$ mixing	.17(.07)	30.(18.6)	.85(.34)	.81(.33)	.87(.36)
	.003(.006)	3.2(4.9)	.014(.03)	.014(.03)	.014(.03)

Table 8 . Limits on $a \times 10^{-3}$, x_s, and $l^{\pm}_{1,2,3} \times 10^{-4}$ for variable m_t. For each constraint, we specify the 1%(10%) upper limits on the first line, and the 1%(10%) lower limits on the second line.

6. Conclusions

We have seen that the recent Argus mixing results, and to a lesser extent the recent ϵ'/ϵ result, put severe constraints on the asymmetries signalling CP violation. A large part of the apparent weakness of the constraint from ϵ'/ϵ lies in theoretical uncertainties. For $m_t = 60$ GeV, in the standard model constrained only by the known value of ϵ, we expect $a < 16.(8.5) \times 10^{-3}$ to 99%(90%) confidence level. With the ϵ'/ϵ constraint as well, we expect $a < 8.9(5.3) \times 10^{-3}$. Finally, with the mixing constraint, we have $a < 2.17(1.52) \times 10^{-3}$. With the ϵ and mixing constraints imposed, the ϵ'/ϵ contraint gives no further information, given the theoretical uncertainties in the calculation.

For larger m_t, the ϵ and ϵ'/ϵ contraints no longer reduce a. However the mixing constraint is still significant: $a < 7.4(2.8) \times 10^{-3}$ before all constraints; $a < 1.45(.82) \times 10^{-3}$ after all constraints. If we randomize m_t between 40 GeV and 180 GeV we find $a < 15.(4.5) \times 10^{-3}$ before constraints and $a < 1.6(.85) \times 10^{-3}$ after constraints. Randomizing m_t also allows us to determine limits on m_t: after all constraints, $m_t > 53.(77.)$ to 99%(90%) confidence level.

Since the lepton asymmetries $l^{\pm}$ are proportional to the product of a and x, the mixing constraint does not greatly affect $l^{\pm}$. However, the ϵ constraint tends to decrease these asymmetries by a factor of two or three; a typical value is $l_1^{\pm} < 3.(2.) \times 10^{-4}$, where $l_1^{\pm}$ is the lepton asymmetry in the incoherent case.

Finally, we consider in passing the effect of the recent observations by Argus of a number of B decay events with no charmed particles in the final state, i.e. $B \to p\bar{p}\pi^+(\pi^-)$.

According to the Argus collaboration the number of observed events implies the inequality $|V_{ub}/V_{cb}| > 0.07$, which is equivalent to $R > 0.3$. Thus, we have also considered input distributions where we replace

$$R = 0. \text{ to } 0.9$$

by

$$R = .3 \text{ to } 0.9.$$

We find that that this change tends to slightly raise our upper limits on a, by at most about 10%.

REFERENCES

1. I. I. Bigi and A. I. Sanda, Nucl. Phys. B193 (1981) 85.
2. A. B. Carter and A. I. Sanda, Phys. Rev. D23 (1981) 1567.
3. J. S. Hagelin, Nucl. Phys. B193 (1981) 123.
4. A.J. Buras, W. Slominski and H. Steger, Nucl. Phys. B245 (1984) 369.
5. Argus Collaboration, DESY report DESY 87-029, 1987.
6. I. Mannelli, in *The 1987 International Symposium on Lepton and Photon Interactions at High Energies*, Hamburg, Germany, 1987 (to be published).
7. A. Pais and S. B. Treiman, Phys. Rev. D12 (1975) 2744.
8. This assumption is implicit in most references, and discussed explicitly, for example, in ref. 7.
9. N. Cabibbo, Phys. Rev. Lett. 10 (1963) 531; M. Kobayashi and T. Maskawa, Progr. Theor. Phys. 49 (1973) 652.
10. L. Maiani, in *Proceedings of the International Symposium on Lepton and Photon Interactions at High Energies*, Hamburg, Germany, 1977; L. Wolfenstein, Phys. Rev. Lett. 51 (1983) 1945.
11. A.J. Buras, W. Slominski and H. Steger, Nucl. Phys. B238 (1984) 529.
12. F. J. Gilman and J. S. Hagelin, Phys. Lett. 126B (1983) 111.
13. G. Altarelli and P. J. Franzini, CERN Report, CERN-TH. 4745/87 (1987).
14. J. Ellis, J. S. Hagelin, and S. Rudaz, CERN Report, CERN-TH. 4679/87 (1987); J. Maalampi and M. Roos, Univ. of Helsinki Report, HU-TFT-87-12 (1987); V. Barger et al., Univ of Wisconsin-Madison Report, MAD/PH/341 (1987); L.-L. Chau and Q.-Y. Keung, UC Davis Report, UCD-87-02; H. Harari and Y. Nir, SLAC Report, SLAC-PUB-4341 (1987); and so on.
15. S. L. Wu, in *The 1987 International Symposium on Lepton and Photon Interactions at High Energies*, Hamburg, Germany, 1987 (to be published).
16. Wolfenstein, Ref. 10

FIGURE CAPTIONS

1. Scatter plot of a versus x for randomized standard model parameters. The dashed lines indicate the Argus limits on x.
2. Histogram of a for: no constraints (solid); ϵ and ϵ'/ϵ constraints (dashed); ϵ and mixing constraints (dotted). $m_t = 45$ GeV.
3. Histogram of a for: no constraints (solid); ϵ and ϵ'/ϵ constraints (dashed); ϵ and mixing constraints (dotted). $m_t = 80$ GeV.
4. Histogram of m_t for: ϵ constraint alone (solid); ϵ and ϵ'/ϵ constraints (dashed); ϵ and mixing constraints (dotted).

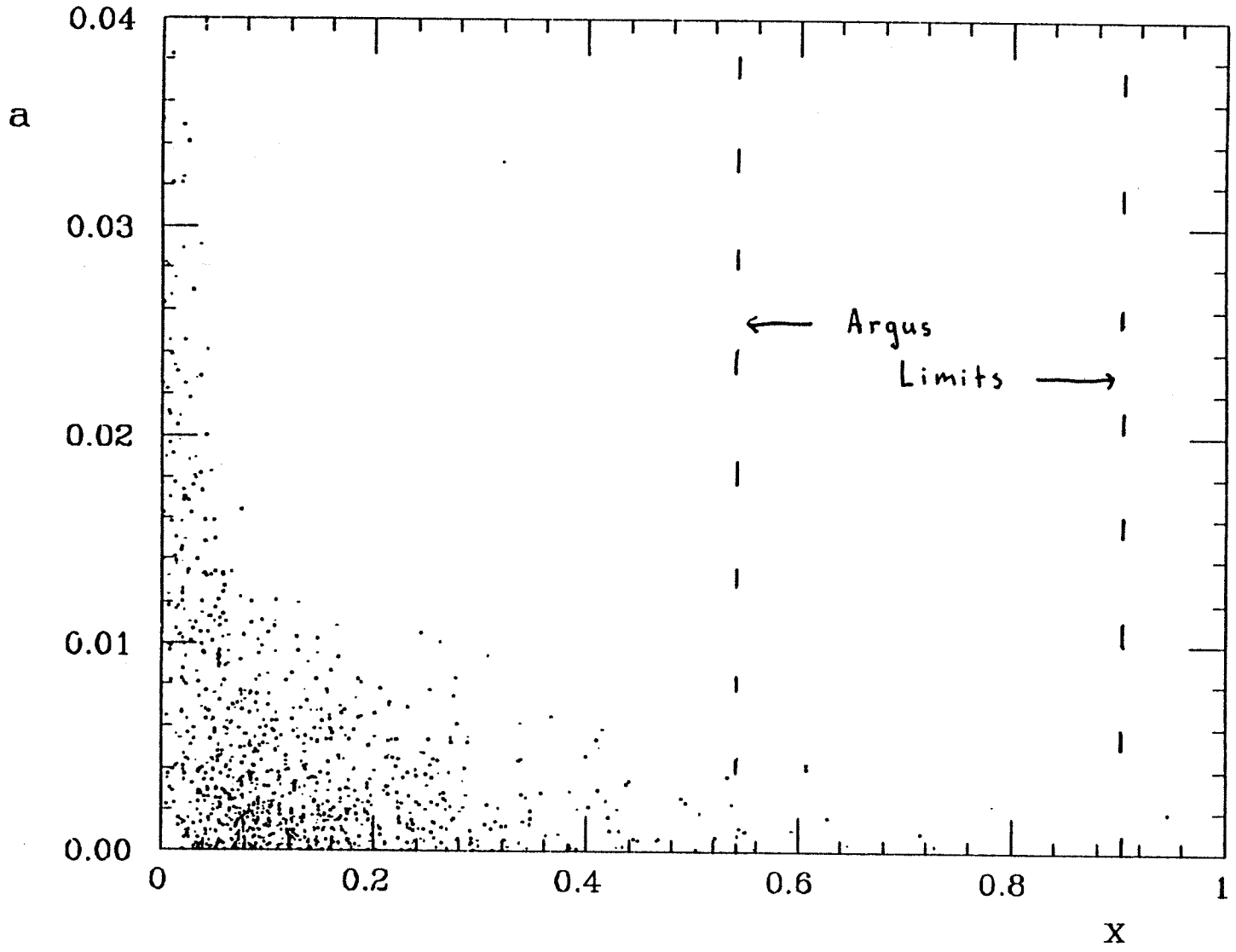

Fig. 1

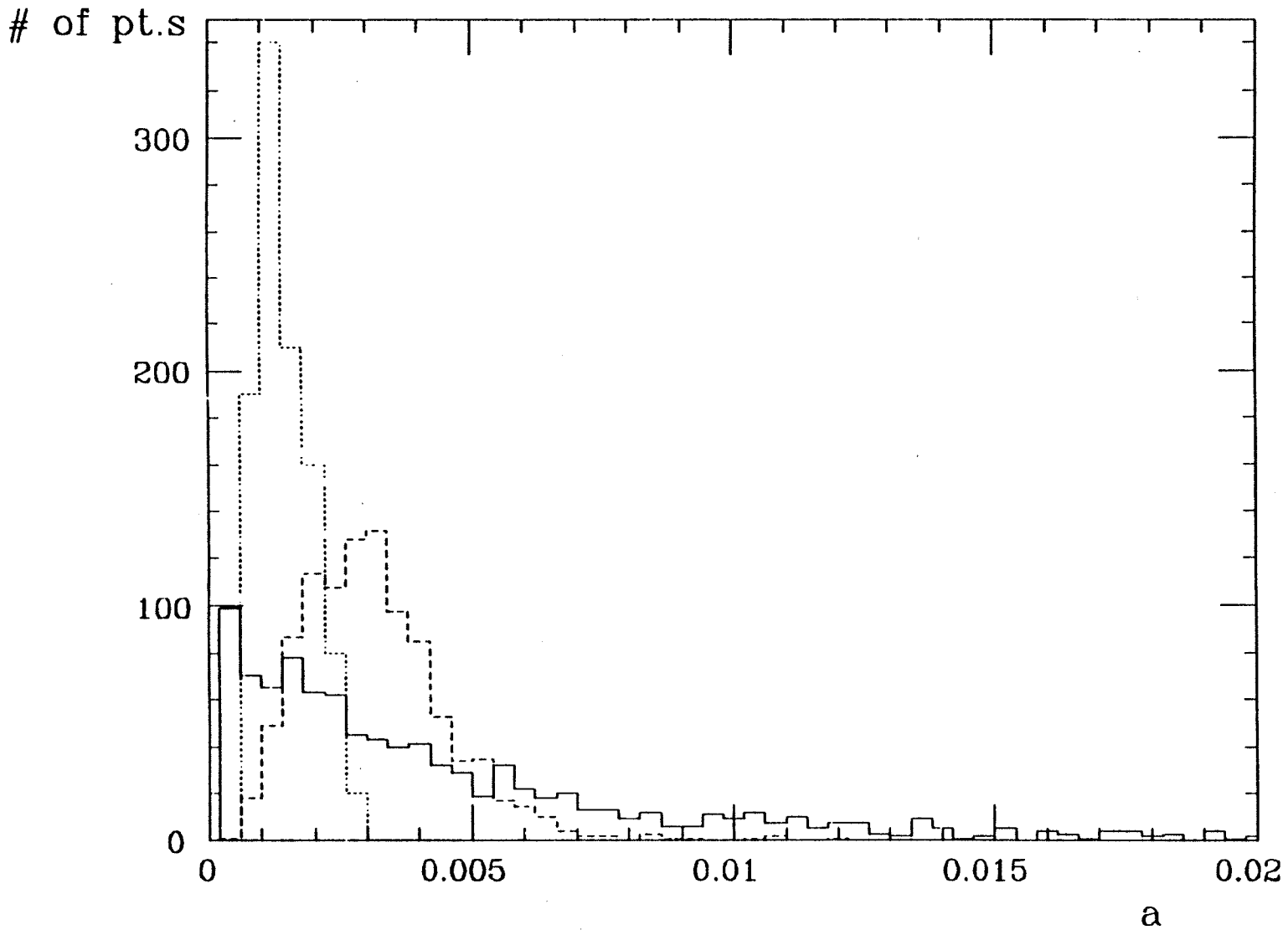

Fig. 2

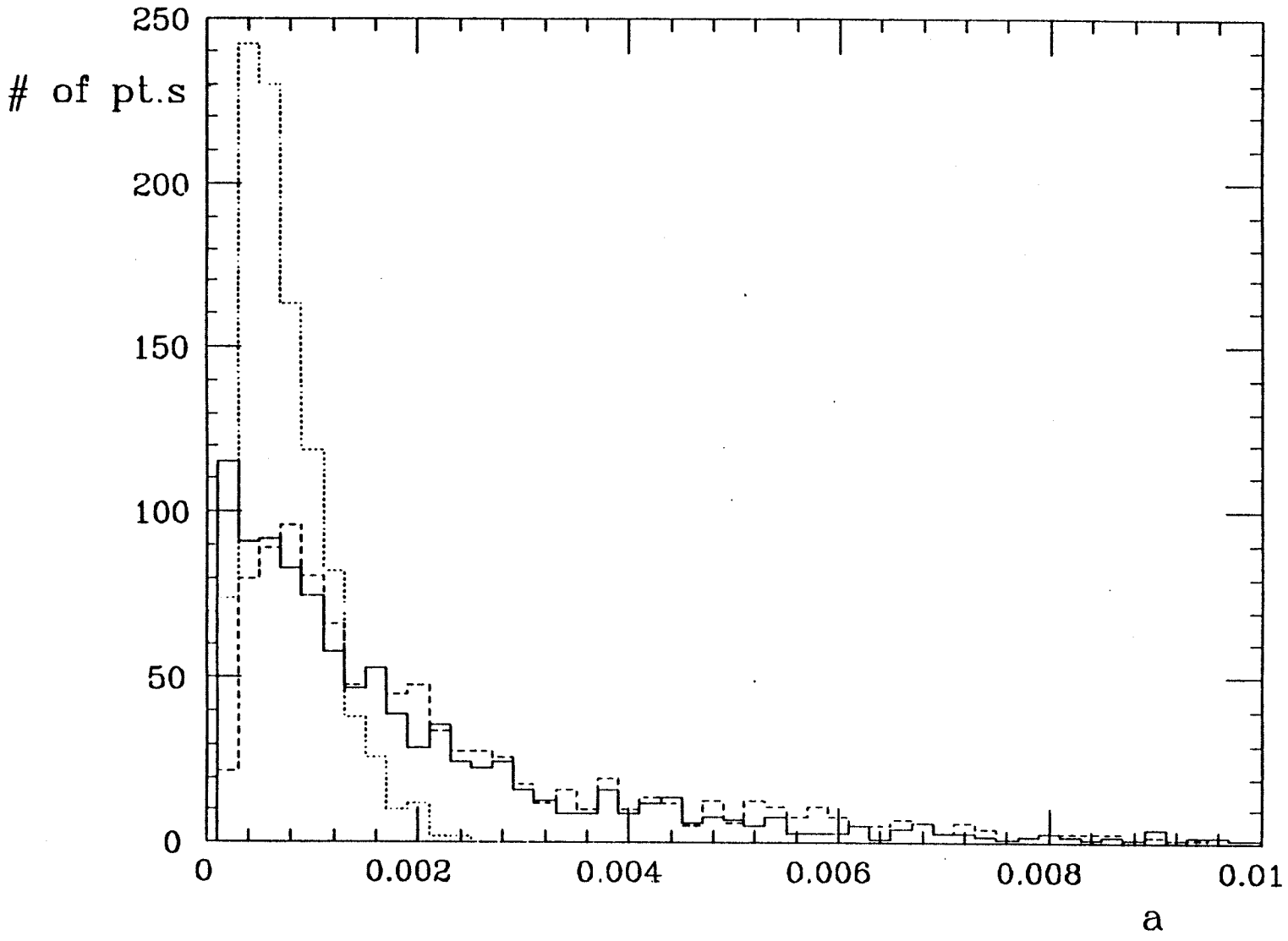

Fig. 3

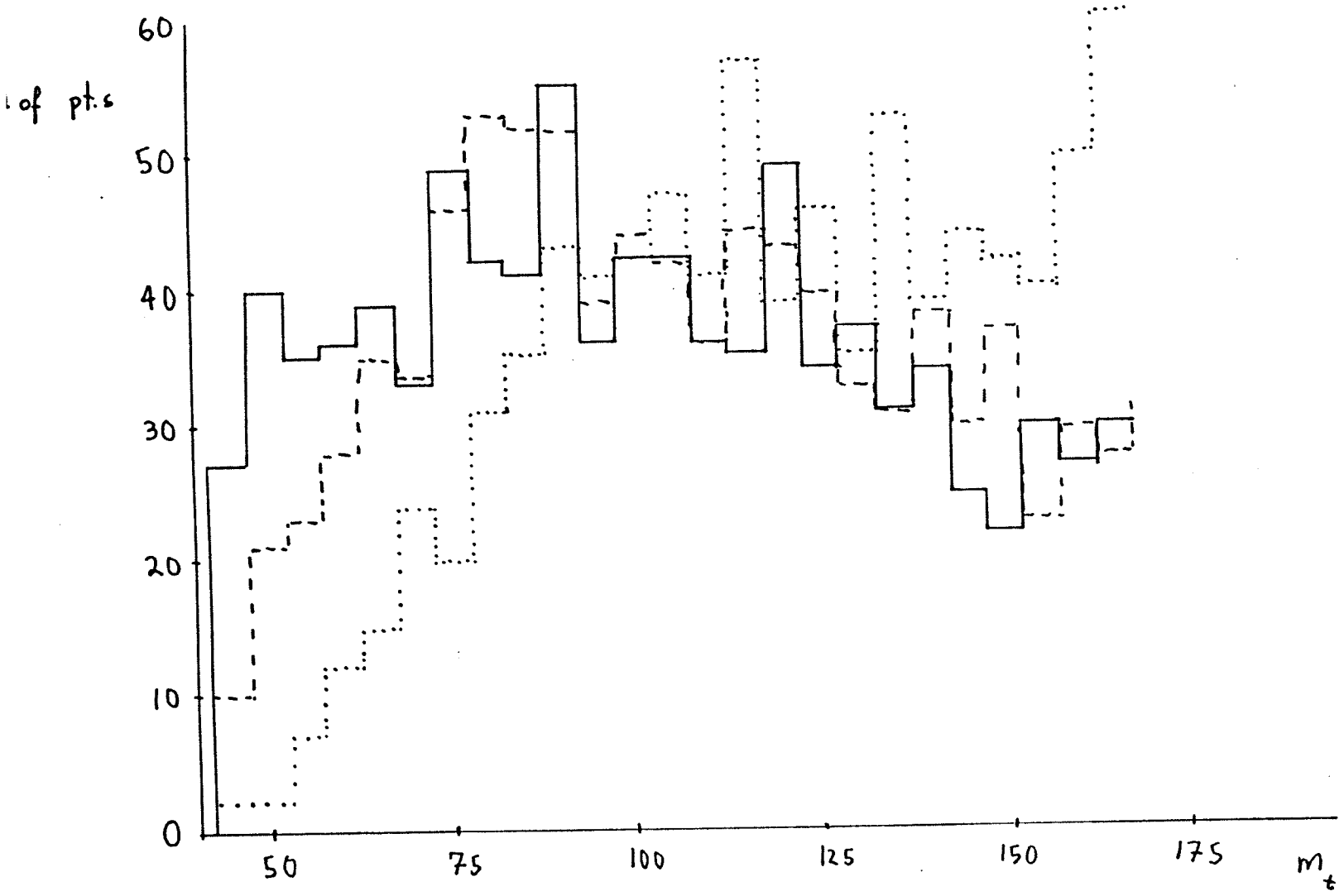

Fig. 4